WILEY | Hindawi

Research Article

A Comparative Study of Natural Convection Flow of Fractional Maxwell Fluid with Uniform Heat Flux and Radiation

Ruihua Tang [ID],[1] Sadique Rehman [ID],[2] Aamir Farooq [ID],[3] Muhammad Kamran [ID],[4] Muhammad Imran Qureshi [ID],[5] Asfand Fahad [ID],[5] and Jia-Bao Liu [ID][6]

[1]*College of Electronic Engineering, Chaohu University, Hefei 238024, China*
[2]*Department of Mathematics, Islamia College Peshawar, Peshawar 25000, Pakistan*
[3]*Department of Mathematics, Abbottabad University of Science and Technology, Abbottabad, Pakistan*
[4]*Department of Mathematics, COMSATS University Islamabad, Wah Campus, Wah Cantt 47040, Pakistan*
[5]*Department of Mathematics, COMSATS University Islamabad, Vehari Campus, Vehari 61100, Pakistan*
[6]*School of Mathematics and Physics, Anhui Jianzhu University, Hefei 230601, China*

Correspondence should be addressed to Muhammad Kamran; getkamran@gmail.com

This paper focuses on the comparative study of natural convection flow of fractional Maxwell fluid having uniform heat flux and radiation. The well-known Maxwell fluid equation with an integer-order derivative has been extended to a non-integer-order derivative, i.e., fractional derivative. The explicit expression for the temperature and velocity is acquired by utilizing the Laplace transform (LT) technique. The two fractional derivative concepts are used (Caputo and Caputo–Fabrizio derivatives) in the formulation of the problem. Utilizing the Mathcad programming, the effect of certain embedded factors and fractional parameters on temperature and velocity profile is graphically presented.

1. Introduction

To specify the performance of non-Newtonian fluids, numerous models have been applied. The Maxwell fluid is the first viscoelastic rate type fluid, which is also extensively utilized. The differential form and rate type models have gotten a lot of attention among them. In recent years, this model has shown some achievements in portraying the reactions of some polymeric liquids. In industry and engineering, viscoelastic fluids pass through many processes, such as synthetic propellants and so on. Because of the simplicity of the Maxwell fluid, many investigators are paying particular attention to it [1–4]. Khan et al. [5] researched on heat transfer of Maxwell fluid through an infinite vertical plate. In this study, they obtained the analytical solutions for temperature and velocity via LT. Such a model was studied by Khan et al. [6] using fractional CF derivative.

The subject of fractional calculus is as old as standard calculus. Fractional calculus began when L' Hospital wrote

to Leibnitz about the significance of $d^n y/dx^n$ when $n = 1/2$. Leibnitz replied in 1695 saying that it might be an apparent paradox from which one day useful repercussions would be drawn. Between the 17th century and the early 20th century, the subject of fractional calculus stayed more or less dormant. The subject matter has been found in applications in all kinds of problems in various fields over the last few years, like fluid flow, reaction, diffusion, relaxation, rheology, reaction-diffusion, oscillation, anomalous diffusion, physics, electrical network, chemistry, dynamical problems, and so on. Nowadays, many researchers are using the concept of fractional derivative because fractional-order differential equation solutions define real-life situations effectively than the solution obtained through the corresponding integer-order differential equations. Aman et al. [7] discussed about heat, velocity, and shear stress of fractional Maxwell model in a flexible medium using numerical LT. The semianalytical solutions for Maxwell fluid with fractional derivative were discussed in [8, 9]. The solutions for generalized Maxwell

fluid using Fourier and Laplace transform can be determined by Fetecau et al. [10]. Maxwell nanofluids were examined by Aman et al. [11] using four distinct molecular liquids. The impact of second-order fractional Maxwell (MHD) fluid was investigated by Liu and Guo [12].The flow of Maxwell fluid with MHD effects flowing over a stretching sheet was investigated numerically by Shateyi and Marewo [13]. Mohi [14] discussed the closed-form solution of fractional Maxwell of MHD effects using Laplace and Fourier transform. The comparative research was performed in [15] on MHD Maxwell fluid with Newtonian heating on a boundary layer. Abro and Shaikh [16] investigated the analytical solutions for Maxwell fluid over a vibratory plane. Asjad et al. [17] presented the comparisons between Caputo and Caputo–Fabrizio fractional derivatives on second-grade fluid over Newtonian heating. Raza and Ullah [18] used the fractional Maxwell fluid to compare the fractional derivatives of C and CF using the Laplace transformation. Maxwell fluid's natural convection between two parallel plates was discussed by Wang et al. [19]. The exact solution for Maxwell MHD fluid in a perforated medium was obtained by Khan et al. [20]. Zheng et al. [21] investigated extended Maxwell flow due to a vibratory and uniform moving plate. Fetecau et al. [22] used the LT to solve the second problem of Stokes for Maxwell fluids. Farooq et al. [23] presented the MHD Maxwell flow through the infinitely stretched surface of nanomaterials. Many interesting and very useful results related to the cylindrical Maxwell model can be found in [24–27]. The analytical and semianalytical solutions for Maxwell fluid between two moving plates were obtained by Hisham et al. [28]. Free convection flow has many applications in science and engineering like determining heat losses or heat load for heating, ventilating, air conditioning, and so on. Azhar et al. [29] considered the mixed convection flow of fractional nanofluids with uniform heat flux and heat source. Toki [30] examined the natural convection flow of unsteady MHD fluid and found the exact solutions of flow parameters. Fetecau et al. [31] studied the influence of radiation and permeability on MHD flow moving via an oscillating vertical plate with uniform heat flux.

The above literature motivates us to work on the natural convection flow of the fractional Maxwell model. The Caputo and CF fractional derivative approaches are used to determine the solutions. The numerical Laplace transform is utilized for the solutions of velocity and temperature. We see the comparisons between standard-order derivative and fractional-order derivative. Finally, we observe the graphical representation of various embedded parameters like Maxwell fluid factor, fractional parameter, and Grashof and Prandtl numbers.

2. Mathematical Statement

Here, we will assume the unsteady oscillatory natural convection flow of Maxwell fluid under the effects of radiation and uniform heat flux. Initially, with the uniform temperature T_∞, the fluid and the plate are at rest. After some time, at $t = 0^+$, the plate begins to oscillate in x-direction, and its velocity is given by

$$v = UH(t)\text{Cos}(\omega t)i, \quad t > 0. \tag{1}$$

Following are the governing equations for the flow model:

$$\left(1 + \lambda_1 \frac{\partial}{\partial t}\right)\frac{\partial u}{\partial t} = v\frac{\partial^2 u}{\partial y^2} + \left(1 + \lambda_1 \frac{\partial}{\partial t}\right)g\beta(T - T_\infty), \tag{2}$$

$$\frac{\partial T}{\partial t} = \frac{k}{\rho c_p}\frac{\partial^2 T}{\partial y^2} - \frac{1}{\rho c_p}\frac{\partial q_r}{\partial y}, \tag{3}$$

$$\left(1 + \lambda_1 \frac{\partial}{\partial t}\right)\tau(y, t) = \mu\frac{\partial^2 u}{\partial y^2}. \tag{4}$$

Appropriate initial-boundary conditions are

$$u(y, 0) = 0, \quad T(y, 0) = T_\infty, y > 0,$$

$$u(0, t) = UH(t)\text{Cos}(\omega t), \quad \frac{\partial T(0, t)}{\partial y} = -\frac{q_1}{k}, t > 0, \tag{5}$$

$$u(\infty, t) = 0, \quad T(\infty, t) = T_\infty, t > 0.$$

Using Rosseland approximations [22, 30–32] and accepting the small temperature variation among the temperature T_∞ of the free stream and the fluid temperature T, utilizing the Taylor theorem on T^4 at T_∞, and ignoring the second- and higher-order terms, we obtain

$$q_r = -\frac{4\sigma^*}{3\kappa^*}\frac{\partial T^4}{\partial y}, \tag{6}$$

and

$$T^4 \cong 4T_\infty^3 T - 3T_\infty^4, \tag{7}$$

where σ^*, κ^* are, respectively, the Stefan Boltzman constant and the mean absorption coefficient.

Substituting (7) into (6) and then into (3), we obtain (see [30, 32]) the following form:

$$\rho c_p\frac{\partial T}{\partial t} = k\frac{\partial^2 T}{\partial y^2} + \frac{16\sigma^* T_\infty^3}{3\kappa^*}\frac{\partial^2 T}{\partial y^2}. \tag{8}$$

Now, we will make use of the following similarity transformations in order to reduce equations (2), (4), and (8) into the dimensionless form

$$u^* = \frac{u}{U},$$

$$t^* = \frac{U^2}{v}t,$$

$$\omega^* = \frac{v}{U^2}\omega,$$

$$\zeta^* = \frac{U}{v}y,$$

$$\lambda = \frac{U^2}{v}\lambda_1,$$

$$S = \frac{Uk}{\nu q_1}(T - T_\infty),$$

$$\Pr = \frac{\mu c_p}{k},$$

$$Gr = \left(\frac{\nu}{U^2}\right)^2 \frac{g\beta q_1}{k},$$

$$Nr = \frac{16\sigma^* T_\infty^3}{3k\kappa^*},$$

$$\psi^* = \frac{\nu}{\mu U^2}\tau. \tag{9}$$

Substituting the above dimensionless parameters into equations (2), (4), and (8) and removing * from $u, t, \omega, \psi,$ and ζ, we get the following forms:

$$\left(1 + \lambda\frac{\partial}{\partial t}\right)\frac{\partial u(\zeta,t)}{\partial t} = \frac{\partial^2 u(\zeta,t)}{\partial \zeta^2} + \left(1 + \lambda\frac{\partial}{\partial t}\right)GrS(\zeta,t), \tag{10}$$

$$\Pr\frac{\partial S}{\partial t} = (1 + Nr)\frac{\partial^2 S(y,t)}{\partial \zeta^2}, \quad \zeta, t > 0, \tag{11}$$

$$\left(1 + \lambda\frac{\partial}{\partial t}\right)\psi(\zeta,t) = \frac{\partial u(\zeta,t)}{\partial \zeta}. \tag{12}$$

To obtain the fractional model, we replace the inner time derivative by the time fractional derivative and we acquire a set of fractional PDEs as follows:

$$\left(1 + \lambda D_t^\alpha\right)\frac{\partial u(\zeta,t)}{\partial t} = \frac{\partial^2 u(\zeta,t)}{\partial \zeta^2} + \left(1 + \lambda D_t^\alpha\right)GrS(\zeta,t), \tag{13}$$

$$\Pr D_t^\alpha S = (1 + Nr)\frac{\partial^2 S(\zeta,t)}{\partial \zeta^2}, \quad \zeta, t > 0, \tag{14}$$

$$\left(1 + \lambda D_t^\alpha\right)\psi(\zeta,t) = \frac{\partial u(\zeta,t)}{\partial \zeta}. \tag{15}$$

By neglecting the * sign and utilizing equation (9), we will get the following initial and boundary conditions:

$$u(\zeta, 0) = 0,$$

$$\theta(\zeta, 0) = 0,$$

$$u(0, t) = H(t)\mathrm{Cos}(\omega t),$$

$$\frac{\partial S(0,t)}{\partial \zeta} = -1, \tag{16}$$

$$u(\zeta, t) = 0,$$

$$S(\zeta, t) = 0, \quad \zeta \longrightarrow \infty.$$

3. Preliminaries

3.1. Caputo Fractional Derivative. The Caputo fractional derivative is given by

$$^C D_t^\chi f(y,t) = \begin{cases} \dfrac{1}{\Gamma(1-\chi)}\displaystyle\int_0^t (t-\nu)^{-\chi} f'(y,\nu)\mathrm{d}\nu, & 0 \le \chi < 1, \\[2mm] \dfrac{\partial f(y,t)}{\partial t} & \chi = 1. \end{cases} \tag{17}$$

The LT of Caputo fractional derivative is given by

$$L\left\{^C D_t^\chi g(y,t)\right\} = q^\chi L\{g(y,t)\} - q^{\chi-1}g(y,0). \tag{18}$$

3.2. Caputo–Fabrizio Fractional Derivative. The Caputo–Fabrizio fractional derivative is given by

$$^{CF} D_t^\chi g(y,t) = \begin{cases} \dfrac{1}{(1-\chi)}\displaystyle\int_0^t e^{(-\chi(t-\nu)/(1-\chi))} g\prime(y,\nu)\mathrm{d}\nu, & 0 \le \chi < 1, \\[2mm] \dfrac{\partial g(y,t)}{\partial t} & \chi = 1. \end{cases} \tag{19}$$

The LT of Caputo–Fabrizio fractional derivative is defined by the following formula:

$$L\left\{^{CF} D_t^\chi g(y,t)\right\} = \frac{qL\{g(y,t)\} - g(y,0)}{(1-\chi)q + \chi}. \tag{20}$$

Remark. If $\chi \longrightarrow 1$, then we obtain

$$\lim_{\chi \longrightarrow 1} L\left\{^C D_t^\chi g(y,t)\right\} = \lim_{\chi \longrightarrow 1} L\left\{^{CF} D_t^\chi g(y,t)\right\} = qL\{g(y,t)\}$$

$$- g(y,0) = L\left\{\frac{\partial g(y,t)}{\partial t}\right\}. \tag{21}$$

4. Temperature Profile with Caputo Derivative

Taking the LT of equation (14) and utilizing the corresponding ICs and BCs, we obtain the following form:

$$\overline{S}(\zeta, q) = \frac{1}{q\sqrt{q^\alpha \Pr_{\mathrm{eff}}}} e^{-y\sqrt{q^\alpha \Pr_{\mathrm{eff}}}}, \quad \text{where } \Pr_{\mathrm{eff}} = \frac{\Pr}{1 + Nr}. \tag{22}$$

The inverse LT of equation (22) is given by convolution product:

$$S(\zeta,t) = \frac{1}{\sqrt{\text{Pr}_{\text{eff}}}} \int_0^t [\theta_1(t-\psi) * \theta_2(\zeta,\psi)]\mathrm{d}\psi, \qquad (23)$$

where

$$\theta_1(t) = L^{-1}\left\{\frac{1}{\sqrt{q^\alpha}}\right\} = \frac{t^{-1+(\alpha/2)}}{\Gamma(\alpha/2)},$$

$$\theta_2(\zeta,t) = L^{-1}\left\{\frac{e^{-y\sqrt{\text{Pr}_{\text{eff}}}q^{\alpha/2}}}{q}\right\} = \varphi\left(1, -\frac{\alpha}{2}, -y\sqrt{\text{Pr}_{\text{eff}}}\,t^{-\alpha/2}\right),$$

$$(24)$$

$$\overline{S}(\zeta,q) = \frac{1}{q\sqrt{\text{Pr}_{\text{eff}}(m_0 q/(q+\alpha m_0))}}e^{-y\sqrt{\text{Pr}_{\text{eff}}m_0 q/(q+\alpha m_0)}}, \quad \text{where } m_0 = \frac{1}{1-\alpha}. \qquad (25)$$

Inverse Laplace of equation (25) is obtained through the Faltung theorem, and we have

$$S(\zeta,t) = \int_0^t [g(t-\xi) * h(\zeta,\xi)]\mathrm{d}\xi, \qquad (26)$$

where $g(t) = L^{-1}\{g(q)\} = (1/\text{Pr}_{\text{eff}}m_0)[\delta(t) + m_0\alpha]$ and

$$h(\zeta,t) = L^{-1}\{H(\zeta,q)\}$$

$$= \frac{1}{\pi}H(t)\int_0^{\alpha m_0}\sqrt{\frac{\alpha m_0}{\text{Pr}_{\text{eff}}m_0 - v}}e^{-vt}\text{Cos}\left(y\frac{\alpha m_0}{\text{Pr}_{\text{eff}}m_0 - v}\right)\mathrm{d}v. \qquad (27)$$

6. Nusselt Number

The Nusselt number Nu measures the rate of heat transfer at the plate. The Nusselt number for both equations (22) and (25) is constant:

$$Nu(t) = 1. \qquad (28)$$

7. Temperature Profile in Ordinary Case $\alpha \longrightarrow 1$

Taking LT on equation (11) and utilizing the related initial-boundary conditions, we get

$$\overline{S}(\zeta,q) = \frac{1}{\sqrt{\text{Pr}_{\text{eff}}}q^{3/2}}e^{-\zeta\sqrt{q\text{Pr}_{\text{eff}}}}. \qquad (29)$$

The inverse LT of equation (29) is

where $\varphi(x,y,z) = \sum_{n=0}^{\infty} z^n/(\Gamma(n+1)\Gamma(x+ny)); 0 < \alpha < 1$.

5. Temperature Profile with CF Derivative

Applying LT to equation (14) and introducing equations (19) and (20), we get

$$S(\zeta,t) = \frac{2\sqrt{t}}{\sqrt{\text{Pr}_{\text{eff}}}}\left[\frac{1}{\sqrt{\pi}}e^{\left(-\zeta^2\frac{\text{Pr}_{\text{eff}}}{4t}\right)} - \frac{\zeta\sqrt{\text{Pr}_{\text{eff}}}}{2\sqrt{t}}erfc\left(\frac{\zeta\sqrt{\text{Pr}_{\text{eff}}}}{2\sqrt{t}}\right)\right], \qquad (30)$$

and such solution was obtained by Abro and Shaikh [16].

8. Velocity Profile with Caputo Derivative

Taking LT on equation (13) and related initial-boundary conditions and substituting equation (22) for $\overline{S}(\zeta,q)$, we find that
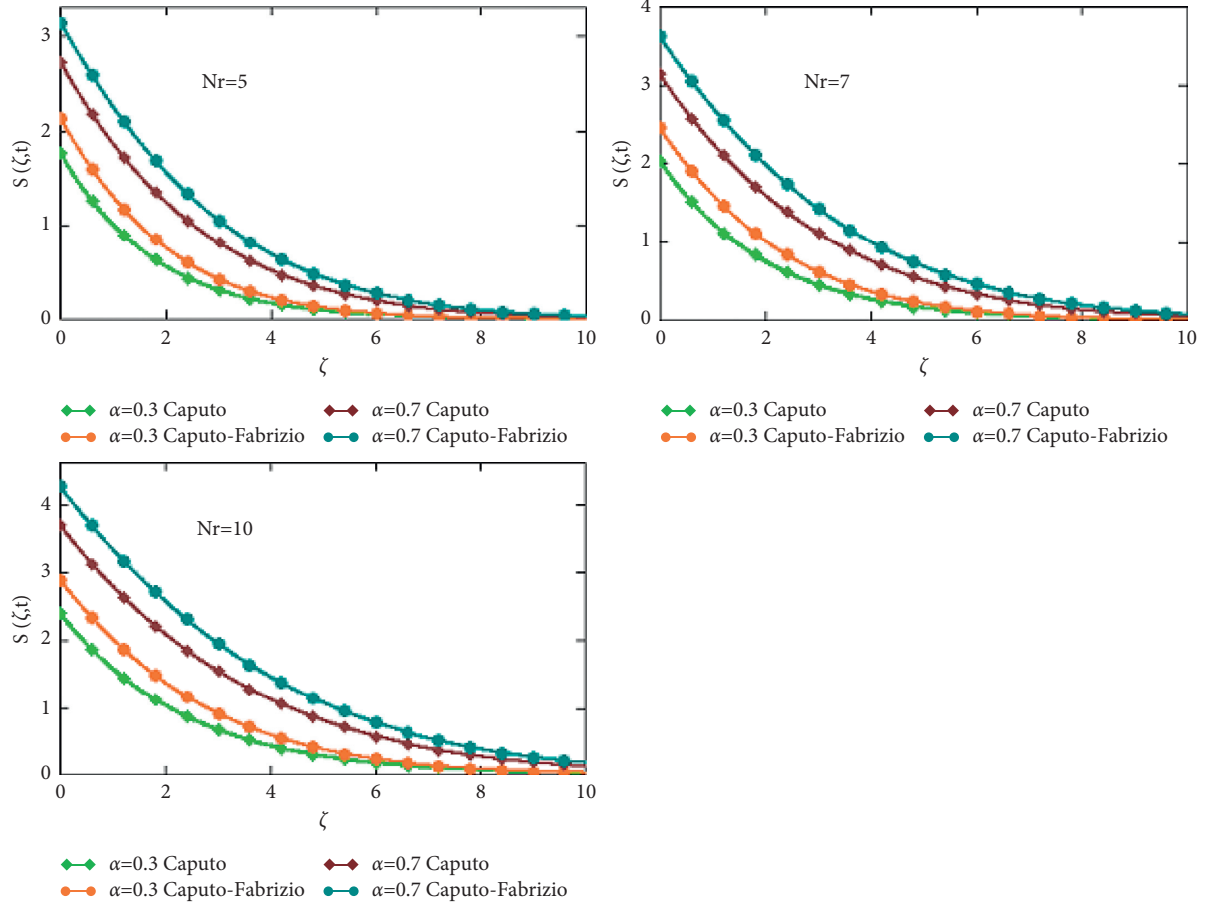
$$\overline{u}(\zeta,q) = \left[\frac{q}{q^2+\omega^2} + \frac{Gr}{\sqrt{\text{Pr}_{\text{eff}}}}\frac{(1+\lambda q^\alpha)}{q\sqrt{q^\alpha}\left[q^\alpha\text{Pr}_{\text{eff}} - (1+\lambda q^\alpha)q\right]}\right]e^{-\zeta\sqrt{(1+\lambda q^\alpha)q}}$$

$$-\left[\frac{Gr}{\sqrt{\text{Pr}_{\text{eff}}}}\frac{(1+\lambda q^\alpha)}{q\sqrt{q^\alpha}\left[q^\alpha\text{Pr}_{\text{eff}} - (1+\lambda q^\alpha)q\right]}\right]e^{-\zeta\sqrt{\text{Pr}_{\text{eff}}q^\alpha}}.$$

$$(31)$$

9. Velocity Profile with CF Derivative

Taking the LT on equation (13) and related initial-boundary conditions and substituting equation (25) for $\overline{S}(\zeta,q)$, we have

$$\overline{u}(\zeta,q) = \left[\frac{q}{q^2+\omega^2} + \frac{Gr}{\sqrt{\text{Pr}_{\text{eff}}}m_0}\frac{(q+m_0\alpha+\lambda q m_0)}{q\sqrt{(q/(q+m_0\alpha))}\left[qm_0\text{Pr}_{\text{eff}} - (q+m_0\alpha+\lambda q m_0)q\right]}\right]e^{-\zeta\sqrt{(q+m_0\alpha+\lambda q m_0)q/(q+m_0\alpha)}}$$

FIGURE 1: Variation of Nr with $Pr = 4$ and $t = 7$.

$$-\left[\frac{Gr}{\sqrt{Pr_{eff}}\,m_0}\,\frac{(q + m_0\alpha + \lambda q m_0)}{q\sqrt{(q/(q + m_0\alpha))}\,[q m_0 Pr_{eff} - (q + m_0\alpha + \lambda q m_0)q]}\right]e^{-\zeta\sqrt{Pr_{eff}\,m_0 q/(q + m_0\alpha)}}. \tag{32}$$

10. Velocity Profile in Ordinary Case $\alpha \longrightarrow 1$

Now taking the Laplace transform on equation (10) and related initial and boundary conditions and also substituting equation (29) for $\overline{S}(\zeta, q)$, we obtain
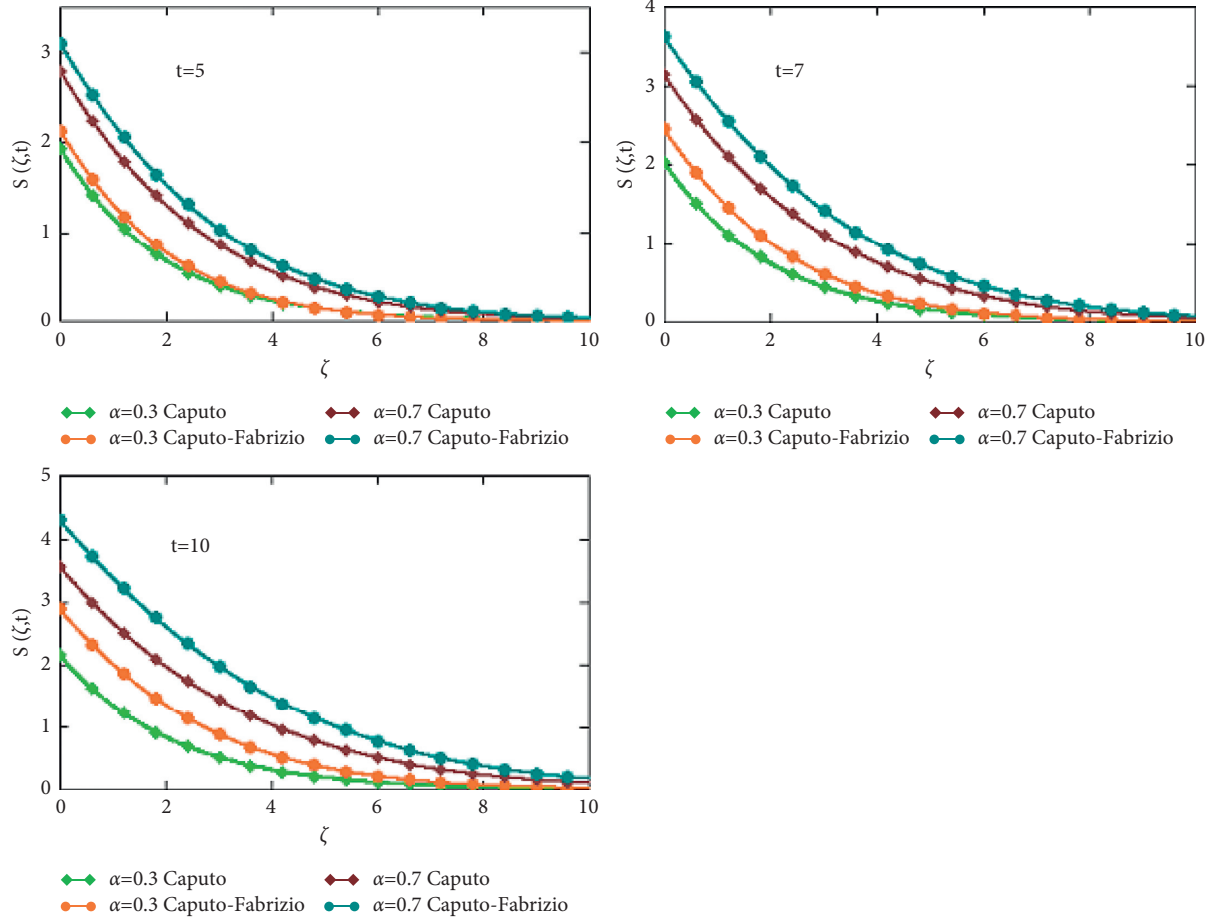
$$\frac{\partial^2 \overline{u}(\zeta, q)}{\partial \zeta^2} - (1 + \lambda q)q\overline{u}(\zeta, q) = -Gr(1 + \lambda q)\frac{1}{\sqrt{Pr_{eff}}\,q^{3/2}}e^{-\zeta\sqrt{q Pr_{eff}}}. \tag{33}$$

On solving the ODE (33), then we acquire

$$\overline{u}(\zeta, q) = \left[\frac{q}{q^2 + \omega^2} + \frac{Gr(1 + \lambda q)}{q^2\sqrt{q}\sqrt{Pr_{eff}}\,[Pr_{eff} - (1 + \lambda q)]}\right]e^{-\zeta\sqrt{q(1 + \lambda q)}}$$

$$- \left[\frac{Gr(1 + \lambda q)}{q^2\sqrt{q}\sqrt{Pr_{eff}}\,[Pr_{eff} - (1 + \lambda q)]}\right]e^{-\zeta\sqrt{q Pr_{eff}}}. \tag{34}$$

We can write equation (34) into the following equivalent form:

$$\overline{u}(\zeta, q) = \frac{q}{q^2 + \omega^2}e^{-\zeta\sqrt{q(1 + \lambda q)}} - \frac{Gr}{\sqrt{Pr_{eff}}}\left[\frac{m_1 - m_2}{m_1^2}\frac{1}{q\sqrt{q}} + \frac{m_2}{m_1}\frac{1}{q^2\sqrt{q}} + \frac{m_2 - m_1}{m_1^2 m_3}\left(\frac{m_3}{\sqrt{q}\left(q - (\sqrt{m_3})^2\right)}\right)\right]e^{-\zeta\sqrt{q(1 + \lambda q)}}$$

$$+ \frac{Gr}{\sqrt{Pr_{eff}}}\left[\frac{m_1 - m_2}{m_1^2}\frac{1}{q\sqrt{q}} + \frac{m_2}{m_1}\frac{1}{q^2\sqrt{q}} + \frac{m_2 - m_1}{m_1^2 m_3}\left(\frac{m_3}{\sqrt{q}\left(q - (\sqrt{m_3})^2\right)}\right)\right]e^{-\zeta\sqrt{q}\sqrt{Pr_{eff}}}, \tag{35}$$

FIGURE 2: Variation of t with Pr = 4 and Nr = 7.

where $m_1 = (1 - \mathrm{Pr_{eff}})/\lambda, m_2 = 1/\lambda, m_3 = (\mathrm{Pr_{eff}} - 1)/\lambda$.

Let

$$M_1(\zeta, q) = e^{-\zeta\sqrt{\mathrm{Pr_{eff}}}\sqrt{q}}. \tag{36}$$
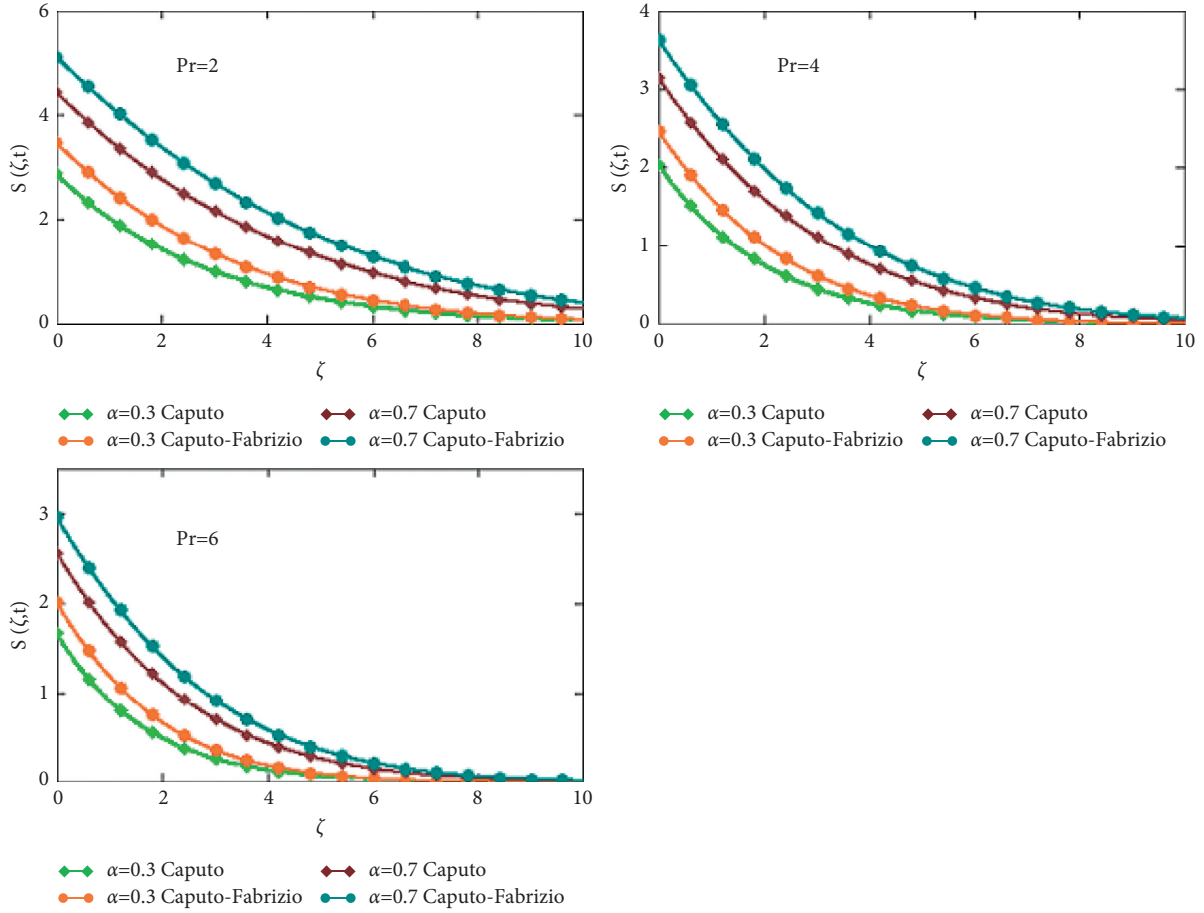
The Laplace inverse of (36) is

$$m(\zeta, t) = L^{-1}\{M_1(\zeta, q)\} = \begin{cases} \dfrac{\zeta\sqrt{\mathrm{Pr_{eff}}}\, e^{-\zeta^2\,(\mathrm{Pr_{eff}}/4t)}}{2t\sqrt{\pi t}}; & \zeta > 0, \\[4mm] \delta(t); & \zeta = 0. \end{cases} \tag{37}$$

$$F(\zeta, q) = e^{-\zeta\sqrt{\lambda}\sqrt{(q+(m_2/2))^2 - (m_2/2)^2}}. \tag{38}$$

Now applying the inverse LT of equation (38), we get

$$f_1(\zeta, t) = \left[m(\zeta, t) + \frac{1}{2\lambda} \int_0^t m(\zeta, w) \frac{w}{\sqrt{t^2 - w^2}} I_1\left(\frac{1}{2\lambda} \sqrt{t^2 - w^2} \right) dw \right] e^{-(1/2\lambda)t}$$

$$= \frac{\zeta\sqrt{t}}{2t\sqrt{\pi t}} e^{\left(-(\zeta^2\lambda/4t) - (1/2\lambda)t \right)} + \frac{1}{2\lambda} e^{-(1/2\lambda)t} \int_0^t \frac{\zeta\sqrt{\lambda}}{2w\sqrt{\pi w}} e^{\left(-\zeta^2\lambda/4w \right)} \frac{w}{\sqrt{t^2 - w^2}} I_1\left(\frac{1}{2\lambda} \sqrt{t^2 - w^2} \right) dw, \tag{39}$$

$$f(\zeta, t) = L^{-1}\{F(\zeta, q)\} = \begin{cases} f_1(\zeta, t); & \zeta > 0, \\[2mm] \delta(t); & \zeta = 0, \end{cases}$$

FIGURE 3: Variation of Pr with $Nr = 7$ and $t = 7$.

Let

$$P(q) = \frac{m_1 - m_2}{m_1^2} \frac{1}{q\sqrt{q}} + \frac{m_2}{m_1} \frac{1}{q^2\sqrt{q}} + \frac{m_2 - m_1}{m_1^2 m_3} \left(\frac{m_3}{\sqrt{q}\left\{ q - \left(\sqrt{m_3}\right)^2 \right\}} \right). \tag{40}$$

Applying the inverse LT of equation (40), we get

$$p(t) = \left[\frac{m_1 - m_2}{m_1^2} 2\sqrt{\frac{t}{\pi}} + \frac{m_2}{m_1} \frac{4t}{3} \sqrt{\frac{t}{\pi}} + \frac{m_2 - a_1}{m_1^2 m_3} e^{m_3 t} erf\left(\sqrt{m_3 t}\right) \right]. \tag{41}$$

Taking the inverse LT on equation (35) and by the convolution theorem, we get

$$u(\zeta, t) = \int_0^t \text{Cos}\omega(t - u) f(\zeta, u) du$$

$$- \frac{Gr}{\sqrt{\text{Pr}_{\text{eff}}}} \int_0^t p(t - u) f(\zeta, u) du \tag{42}$$

$$+ \frac{Gr}{\sqrt{\text{Pr}_{\text{eff}}}} \int_0^t p(t - u) m(y, u) du.$$

11. Shear Stress with Caputo Time Fractional Derivative

Taking Laplace transform on (15), we acquire

$$\overline{\psi}(\zeta, q) = \frac{1}{(1 + \lambda q^\alpha)} \frac{\partial \overline{u}(\zeta, q)}{\partial \zeta}. \tag{43}$$

Differentiating (31) w. r. t ζ, we get

$$\frac{\partial \overline{u}(\zeta, q)}{\partial \zeta} = \left[\frac{Gr}{\sqrt{\text{Pr}_{\text{eff}}}} \frac{(1 + \lambda q^\alpha)\sqrt{\text{Pr}_{\text{eff}} q^\alpha}}{q\sqrt{q^\alpha} \left[q^\alpha \text{Pr}_{\text{eff}} - (1 + \lambda q^\alpha) q \right]} \right] e^{-\zeta\sqrt{\text{Pr}_{\text{eff}} q^\alpha}}$$

$$- \left[\frac{q\sqrt{(1 + \lambda q^\alpha) q}}{q^2 + \omega^2} \right.$$

$$+ \frac{Gr}{\sqrt{\text{Pr}_{\text{eff}}}} \frac{(1 + \lambda q^\alpha)\sqrt{(1 + \lambda q^\alpha) q}}{q\sqrt{q^\alpha} \left[q^\alpha \text{Pr}_{\text{eff}} - (1 + \lambda q^\alpha) q \right]} \right] e^{-\zeta\sqrt{(1 + \lambda q^\alpha) q}}. \tag{44}$$
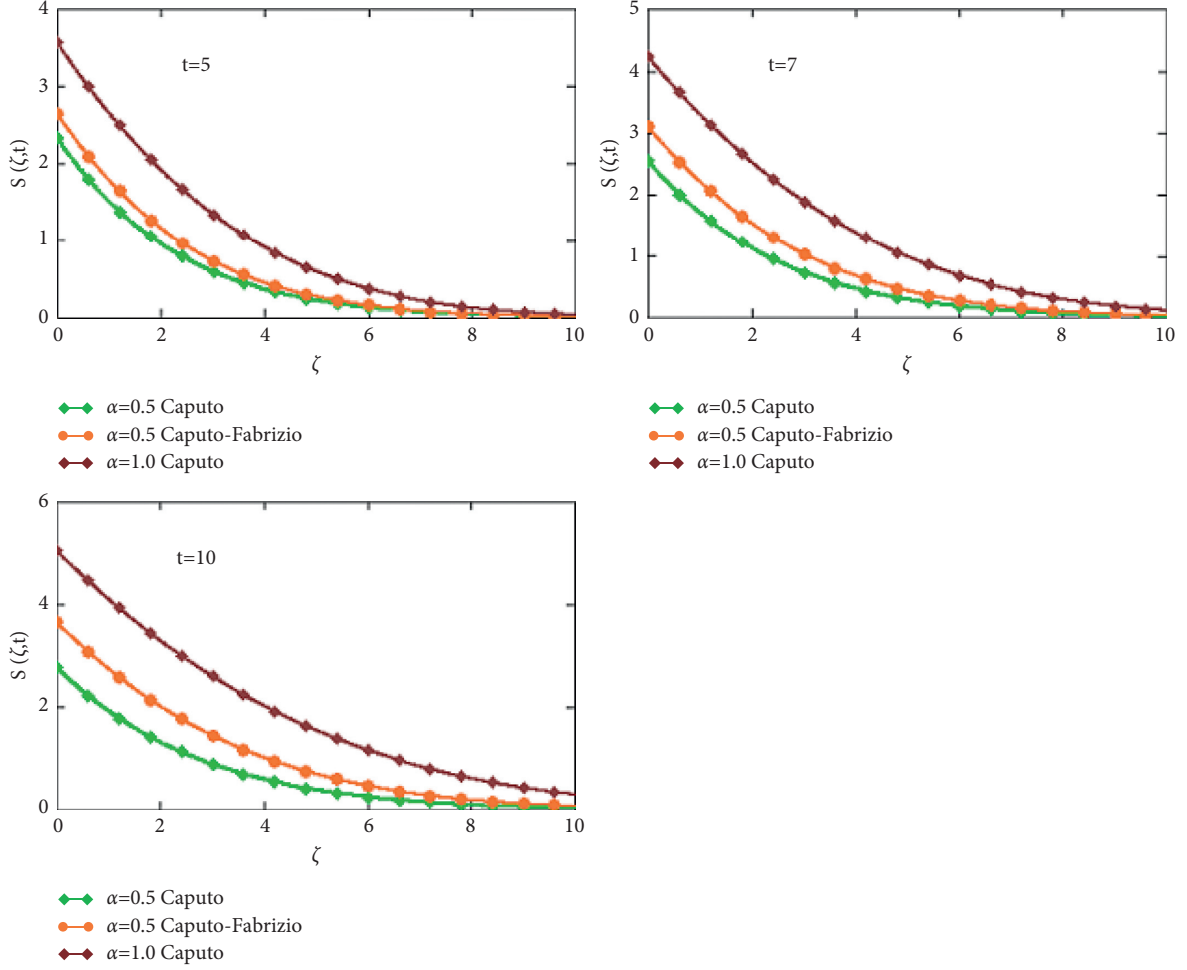
Substituting (44) into (43), we obtain

FIGURE 4: Comparison between fractional model and ordinary model, i.e., $\alpha \longrightarrow 1$.

$$\overline{\psi}(\zeta, q) = \frac{1}{(1 + \lambda q^{\alpha})} \left[\frac{Gr}{\sqrt{\mathrm{Pr_{eff}}}} \frac{(1 + \lambda q^{\alpha}) \sqrt{\mathrm{Pr_{eff}} q^{\alpha}}}{q \sqrt{q^{\alpha}} \left[q^{\alpha} \mathrm{Pr_{eff}} - (1 + \lambda q^{\alpha}) q \right]} \right] e^{-\zeta \sqrt{\mathrm{Pr_{eff}} q^{\alpha}}}$$

$$- \frac{1}{(1 + \lambda q^{\alpha})} \left[\frac{q \sqrt{(1 + \lambda q^{\alpha}) q}}{q^2 + \omega^2} + \frac{Gr}{\sqrt{\mathrm{Pr_{eff}}}} \frac{(1 + \lambda q^{\alpha}) \sqrt{(1 + \lambda q^{\alpha}) q}}{q \sqrt{q^{\alpha}} \left[q^{\alpha} \mathrm{Pr_{eff}} - (1 + \lambda q^{\alpha}) q \right]} \right] e^{-\zeta \sqrt{(1 + \lambda q^{\alpha}) q}}. \tag{45}$$

12. Shear Stress with Caputo–Fabrizio Time Fractional Derivative

Taking LT of Caputo–Fabrizio fractional derivative on (15), we get

$$\overline{\psi}(\zeta, q) = \left(\frac{(q + \alpha m_0)}{q + \alpha m_0 + \lambda q m_0} \right) \frac{\partial \overline{u}(\zeta, q)}{\partial \zeta}. \tag{46}$$

Differentiating (32) w. r. t ζ, we have

$$\frac{\partial \overline{u}(\zeta, q)}{\partial \zeta} = \left[Gr \frac{(q + m_0 \alpha + \lambda q m_0)}{q \left[q m_0 \mathrm{Pr_{eff}} - (q + m_0 \alpha + \lambda q m_0) q \right]} \right] e^{-\zeta \sqrt{\mathrm{Pr_{eff}} m_0 q / (q + m_0 \alpha)}}$$

$$- \left[\frac{q \sqrt{(q + m_0 \alpha + \lambda q m_0) q / (q + m_0 \alpha)}}{q^2 + \omega^2} + \frac{Gr}{\sqrt{\mathrm{Pr_{eff}} m_0}} \frac{(q + m_0 \alpha + \lambda q m_0) \sqrt{(q + m_0 \alpha + \lambda q m_0) q / (q + m_0 \alpha)}}{q \sqrt{q / (q + m_0 \alpha)} \left[q m_0 \mathrm{Pr_{eff}} - (q + m_0 \alpha + \lambda q m_0) q \right]} \right] e^{-\zeta \sqrt{(q + m_0 \alpha + \lambda q m_0) q / q + m_0 \alpha}}. \tag{47}$$
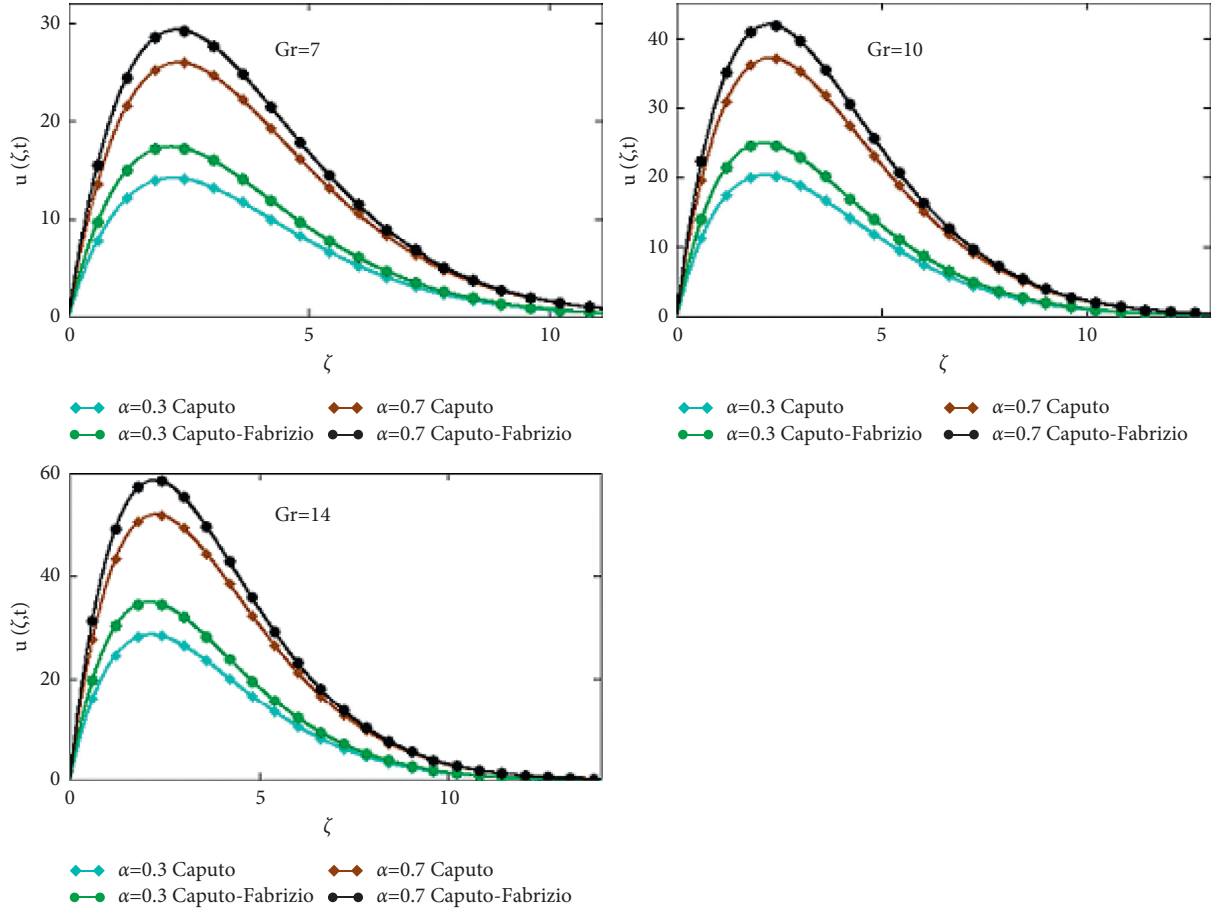
Figure 5: Variation of Gr with $Nr = 7, \lambda = 0.1,$ and $Pr = 4$.

Table 1: Effects of fractional factor α on temperature and velocity profile for CF and C fractional models with $\lambda = 0.1, Gr = 7, Nr = 7, Pr = 4, t = 7,$ and $\omega = \pi/2$.

Parameter α	$S(\zeta, t)$ (CF)	$S(\zeta, t)$ (Caputo)	$u(\zeta, t)$ (CF)	$u(\zeta, t)$ (Caputo)
0.0	0.993	0.993	4.237	4.237
0.1	1.43	1.171	5.749	5.050
0.2	1.732	1.368	7.197	5.954
0.3	2.034	1.585	8.585	6.952
0.4	2.350	1.821	9.915	8.049
0.5	2.622	2.080	11.193	9.250
0.6	2.874	2.362	12.423	10.557
0.7	3.110	2.667	13.608	11.976
0.8	3.331	2.998	14.753	13.510
0.9	3.541	3.356	15.863	15.163
1.0	3.741	3.741	16.939	16.939

Table 2: Effects of ζ on temperature and velocity profile for CF and Caputo fractional models with $\lambda = 0.1, Gr = 7, Nr = 5, Pr = 4, t = 10, \alpha = 0.5,$ and $\omega = \pi/2$.

ζ	$S(\zeta, t)$ (Stehfest)	$S(\zeta, t)$ (Tzou)	$S(\zeta, t)$ (Zakian)	$u(\zeta, t)$ (Stehfest)	$u(\zeta, t)$ (Tzou)	$u(\zeta, t)$ (Zakian)
0.2	2.973	2.961	2.973	5.743	4.551	4.965
0.4	2.785	2.768	2.785	10.628	9.427	10.035
0.6	2.607	2.586	2.607	14.765	13.696	14.326
0.8	2.436	2.415	2.436	18.224	17.356	17.918
1.0	2.274	2.253	2.274	21.070	20.418	20.875
1.2	2.119	2.100	2.119	23.362	22.910	23.259

TABLE 3: Numerical values of temperature profile, velocity profile, and shear stress subjected to various physical factors.

t	Gr	Pr	Nr	λ	$S(\zeta,t)$ (CF)	$u(\zeta,t)$ (CF)	$\psi(\zeta,t)$ (CF)
5	—	—	—	—	2.187	8.250	12.634
7	—	—	—	—	2.622	11.193	17.950
10	—	—	—	—	3.182	16.078	26.449
—	7	—	—	—	—	11.193	17.950
—	10	—	—	—	—	16.032	25.628
—	14	—	—	—	—	22.483	35.866
—	—	2	—	—	3.896	19.035	31.548
—	—	4	—	—	2.622	11.193	17.950
—	—	6	—	—	2.060	8.039	12.571
—	—	—	5	—	2.212	8.865	13.972
—	—	—	7	—	2.622	11.193	17.950
—	—	—	10	—	3.182	14.360	23.413
—	—	—	-	0.1	—	11.193	17.950
—	—	—	-	0.3	—	11.639	18.700
—	—	—	—	0.7	—	12.531	20.197
t	Gr	Pr	Nr	λ	$S(\zeta,t)$ CF	$u(\zeta,t)$ CF	$\psi(\zeta,t)$ CF
5	—	—	—	—	1.879	7.491	11.555
7	—	—	—	—	2.080	9.250	14.874
10	—	—	—	—	2.313	11.915	19.479
-	7	—	—	—	—	9.250	14.874
—	10	—	—	—	—	13.255	21.234
—	14	—	—	—	—	18.596	29.715
—	—	2	—	—	3.119	15.992	26.596
—	—	4	—	—	2.080	9.250	14.874
—	—	6	—	—	1.623	6.572	10.302
—	—	—	5	—	1.746	7.271	11.488
—	—	—	7	—	2.080	9.250	14.874
—	—	—	10	—	2.512	11.960	19.560
—	—	—	—	0.1	—	9.250	14.874
—	—	—	—	0.3	—	9.745	15.656
—	—	—	—	0.7	—	10.714	17.172

TABLE 4: Nomenclature.

u	Velocity of the fluid	S	Temperature of the fluid
U	Amplitude of the fluid	$H(t)$	Heaviside step function
ω	Frequency of oscillation	q_r	Radiative heat flux
g	Gravitational acceleration	λ_1	Maxwell fluid coefficient
c_p	Specific heat at constant pressure	k	Thermal conductivity
β	Volumetric coefficient of thermal expansion	ρ	Fluid density
v	Kinematic viscosity	μ	Absolute viscosity
Pr	Prandtl number	Gr	Grashof number
Nr	Radiation parameter	ψ	Shear stress
C	Caputo	CF	Caputo–Fabrizio
LT	Laplace transform	q	Laplace transform parameter
α	Fractional parameter	t	Time
q_1	Constant heat flux	i	Unit vector in direction of y

Substituting (47) into (46), we obtain the following form:

$$\overline{\psi}(\zeta,q) = \left[Gr \frac{(q+\alpha m_0)}{q\left[qm_0 \mathrm{Pr}_{eff} - (q+m_0\alpha+\lambda qm_0)q\right]}\right] e^{-\zeta\sqrt{\mathrm{Pr}_{eff}m_0 q/(q+m_0\alpha)}}$$

$$- \left[\frac{q(q+\alpha m_0)\sqrt{(q+m_0\alpha+\lambda qm_0)q/(q+m_0\alpha)}}{(q^2+\omega^2)(q+m_0\alpha+\lambda qm_0)} + \frac{Gr}{\sqrt{\mathrm{Pr}_{eff}}m_0} \frac{(q+\alpha m_0)\sqrt{(q+m_0\alpha+\lambda qm_0)q/(q+m_0\alpha)}}{q\sqrt{q/(q+m_0\alpha)}\left[qm_0\mathrm{Pr}_{eff}-(q+m_0\alpha+\lambda qm_0)q\right]}\right]$$

$$\cdot e^{-\zeta\sqrt{(q+m_0\alpha+\lambda qm_0)q/(q+m_0\alpha)}}.$$
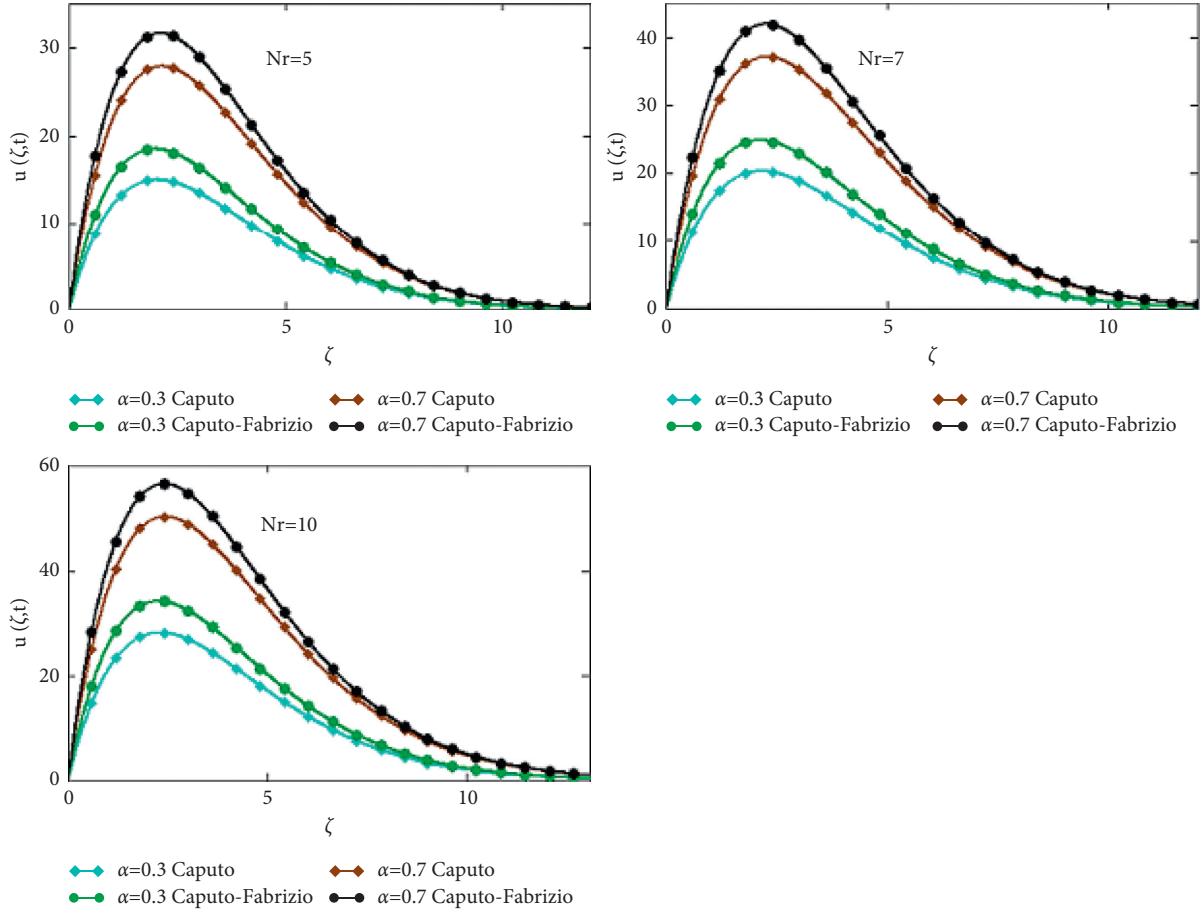
(48)

FIGURE 6: Variation of Nr with $Gr = 10, \lambda = 0.1, t = 7, \mathrm{Pr} = 4,$ and $t = 7$.

13. Shear Stress in Ordinary Case $\alpha \longrightarrow 1$

Taking Laplace transform on equation (12), we get

$$\overline{\psi}(\zeta, q) = \frac{1}{(1 + \lambda q)} \frac{\partial \overline{u}(\zeta, q)}{\partial \zeta}. \tag{49}$$

Differentiating equation (34) w. r. t ζ, we get

$$\frac{\partial \overline{u}(\zeta, q)}{\partial \zeta} = \left[\frac{-q\sqrt{q(1 + \lambda q)}}{q^2 + \omega^2} - \frac{Gr(1 + \lambda q)\sqrt{q(1 + \lambda q)}}{q^2 \sqrt{q} \sqrt{\mathrm{Pr}_{\mathrm{eff}}} \left[\mathrm{Pr}_{\mathrm{eff}} - (1 + \lambda q) \right]} \right] e^{-\zeta \sqrt{q(1 + \lambda q)}} + \left[\frac{Gr(1 + \lambda q)\sqrt{s\mathrm{Pr}_{\mathrm{eff}}}}{q^2 \sqrt{q} \sqrt{\mathrm{Pr}_{\mathrm{eff}}} \left[\mathrm{Pr}_{\mathrm{eff}} - (1 + \lambda q) \right]} \right] e^{-\zeta \sqrt{q\mathrm{Pr}_{\mathrm{eff}}}}. \tag{50}$$

The above equation can be written as

$$\frac{\partial \overline{u}(\zeta, q)}{\partial \zeta} = -\frac{q\sqrt{q(1 + \lambda q)}}{q^2 + \omega^2} e^{-\zeta \sqrt{q(1 + \lambda q)}}$$

$$- \frac{Gr \sqrt{q(1 + \lambda q)}}{\sqrt{\mathrm{Pr}_{\mathrm{eff}}}} \left[\frac{m_1 - m_2}{m_1^2} \frac{1}{q\sqrt{q}} + \frac{m_2}{m_1} \frac{1}{q^2 \sqrt{q}} + \frac{m_2 - m_1}{m_1^2 m_3} \left(\frac{m_3}{\sqrt{q}\left(q - (\sqrt{m_3})^2\right)} \right) \right] e^{-\zeta \sqrt{q(1 + \lambda q)}} \tag{51}$$

$$+ \frac{Gr \sqrt{q\mathrm{Pr}_{\mathrm{eff}}}}{\sqrt{\mathrm{Pr}_{\mathrm{eff}}}} \left[\frac{m_1 - m_2}{m_1^2} \frac{1}{q\sqrt{q}} + \frac{m_2}{m_1} \frac{1}{q^2 \sqrt{q}} + \frac{m_2 - m_1}{m_1^2 m_3} \left(\frac{m_3}{\sqrt{q}\left(q - (\sqrt{m_3})^2\right)} \right) \right] e^{-\zeta \sqrt{q} \sqrt{\mathrm{Pr}_{\mathrm{eff}}}}.$$
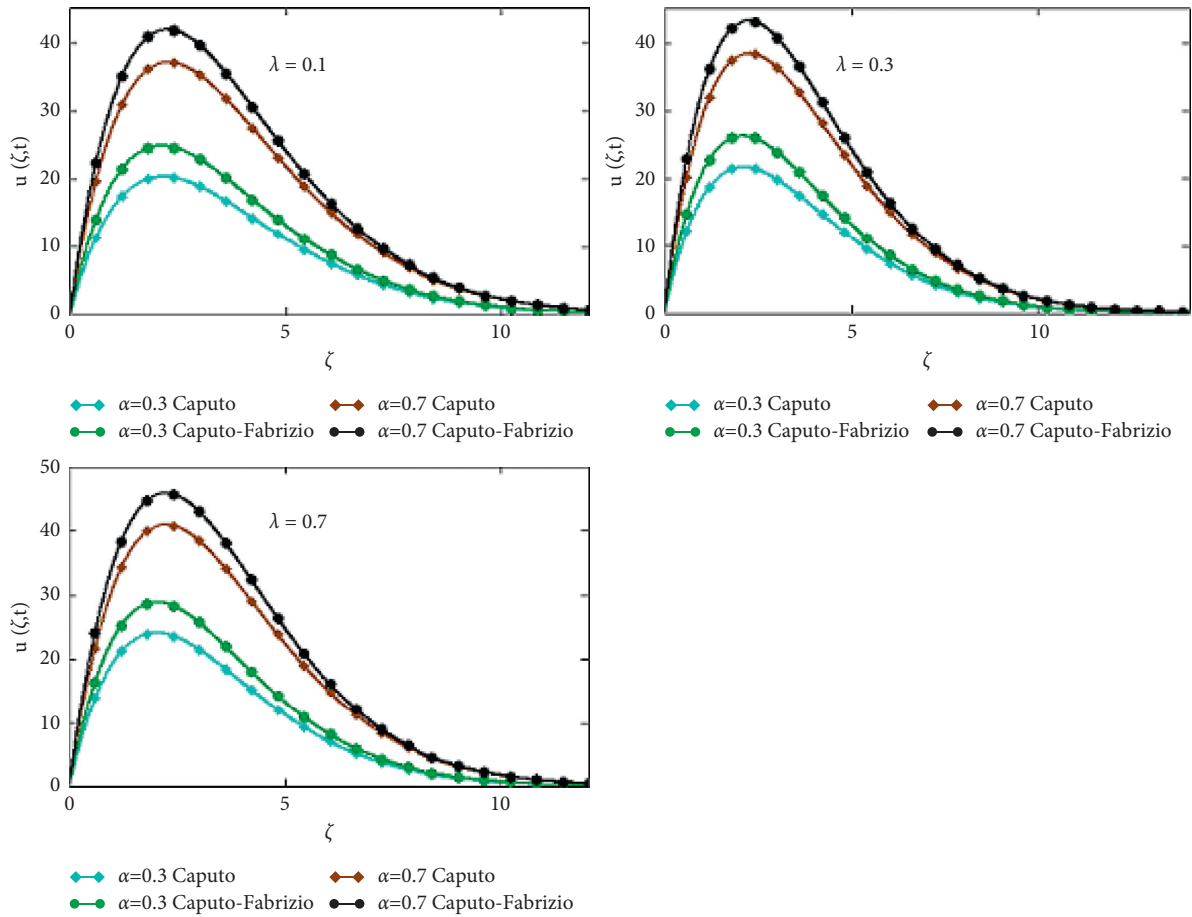
FIGURE 7: Variation of λ with $Nr = 7$, $Gr = 10$, and $\mathrm{Pr} = 4$.

Substituting equation (51) into equation (49), we have

$$\overline{\psi}(\zeta, q) = D(q)F(\zeta, q) - \frac{Gr}{\sqrt{\mathrm{Pr}_{\mathrm{eff}}}} E(q)F(\zeta, q)$$

$$+ \frac{Gr}{\sqrt{\mathrm{Pr}_{\mathrm{eff}}}} K(q)M(\zeta, q), \tag{52}$$

where

$$D(q) = -\frac{q\sqrt{q(1 + \lambda q)}}{(1 + \lambda q)(q^2 + \omega^2)},$$

$$E(q) = \frac{P(q)\sqrt{q(1 + \lambda q)}}{(1 + \lambda q)}, \tag{53}$$

$$K(q) = \frac{G(q)\sqrt{\mathrm{Pr}_{\mathrm{eff}}q}}{(1 + \lambda q)}.$$

Taking the inverse LT on equation (52) and utilizing Faltung theorem, we get

$$\psi(\zeta, t) = D(\zeta, t) * F(\zeta, t) - \frac{Gr}{\sqrt{\mathrm{Pr}_{\mathrm{eff}}}} E(t) * F(\zeta, t)$$

$$+ \frac{Gr}{\sqrt{\mathrm{Pr}_{\mathrm{eff}}}} K(t) * m(\zeta, t). \tag{54}$$

Taking Laplace inverse transform on equation (53), we get

$$D(t) = \frac{\omega}{\lambda} \int_0^t \mathrm{Sin}[\omega(t - h)]e^{(-h/2\lambda)}I_0\left(\frac{h}{2\lambda}\right)\mathrm{d}h,$$

$$E(t) = g(t) * \left[\frac{1}{m_1\lambda\sqrt{\lambda}} \int_0^t I_0\left(\frac{h}{2\lambda}\right)e^{-(-h/2\lambda)}\mathrm{d}h - \frac{1 - m_1\lambda}{m_1\lambda\sqrt{\lambda}} \int_0^t I_1\left(\frac{h}{2\lambda}\right)e^{(-(-h/2\lambda)-m_1(t-h))}\mathrm{d}h\right],$$
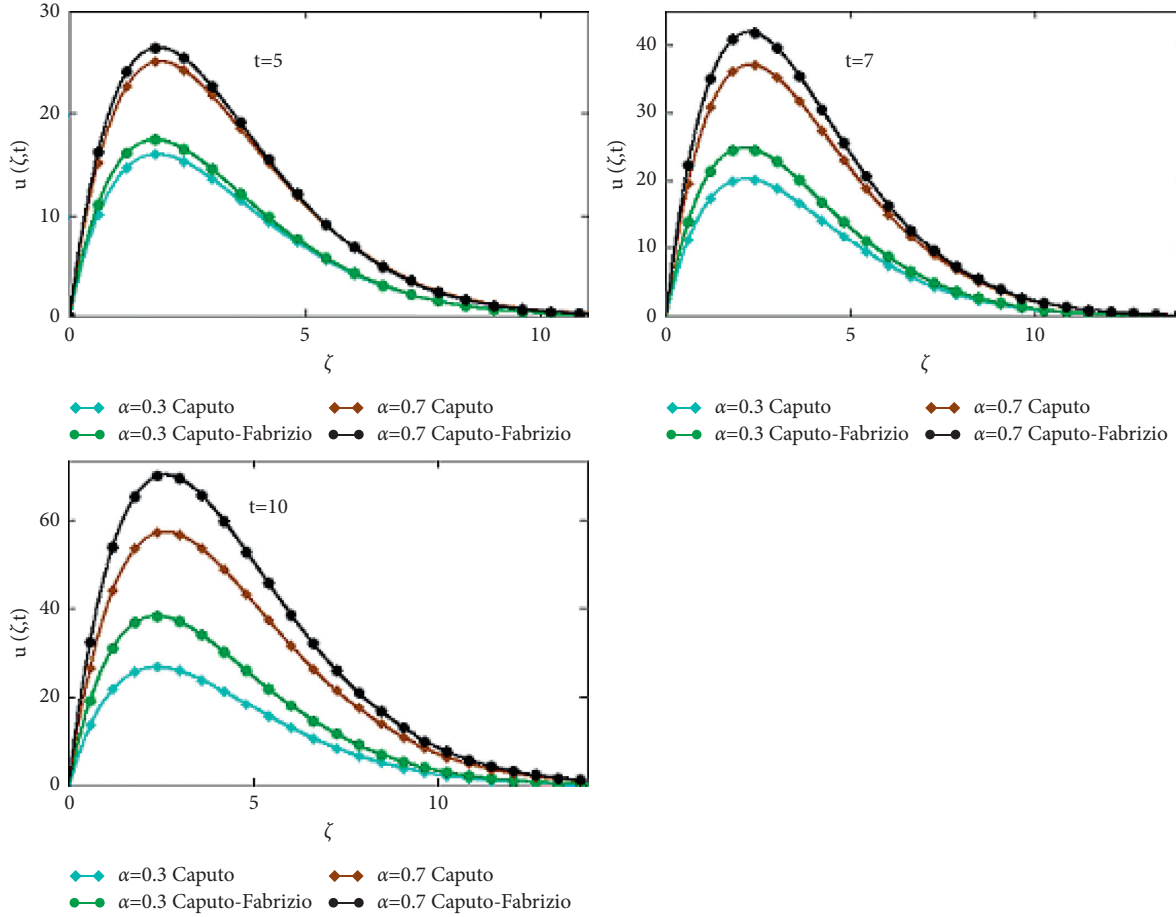
FIGURE 8: Variation of t with $Gr = 10, \lambda = 0.1$, $t = 7$, $Nr = 7$, and $\Pr = 4$.

$$K(t) = g(t) * \left[\frac{m_1\lambda - 1}{m_1^2\lambda} n(t) + \frac{1}{m_1\lambda} \int_0^t n(x)\mathrm{d}x + \frac{m_1\lambda - 1}{m_1^2\lambda} \left[n(t) - m_1 \int_0^t e^{\left[-m_1(t-x) \right]} n(x)\mathrm{d}x \right] \right]. \tag{55}$$

Due to the complex combination of Laplace transform in equations (32), (33), (47), and (50), analytical LP inversion is very difficult, so for the Laplace inversion, we use different numerical LP inversion methods like Stehfest's numerical method, Tzou's algorithms, and Zakian's algorithms.

14. Numerical Discussion and Graphs

The aim of this research is to study the Maxwell fluid's natural convection flow with radiation and consistent heat flow. The differential model is developed into fractional order. There are two fractional derivative concepts that we used (Caputo and Caputo–Fabrizio derivatives). Solutions for temperature and velocity are extended to Caputo and Caputo–Fabrizio derivatives. Solutions are obtained through the Laplace transform method. The effect of various embedded factors on temperature and velocity is a key feature of the model. We are also interested in comparing the Caputo and Caputo–Fabrizio derivative results. Figure 1 shows the behavior of radiation parameter Nr on temperature. The Caputo fractional model

has a smaller temperature as compared to Caputo–Fabrizio. The enhancement of radiation parameter Nr enhances the fluid temperature. The variation of time t on temperature is shown in Figure 2. Figure 2 presents the same behavior of fractional models like Figure 1. The fluid temperature increases with increasing time. Due to this, the boundary layer increases with increasing time. The impact of $\Pr$ is indicated in Figure 3. It is stated that incrementing the Prandtl number $\Pr$ decrements the temperature. Physically, the higher the value of $\Pr$, the higher the fluid viscosity and the lower the thermal conductivity. Because of this, the thickness of the boundary layer falls. Figure 4 shows the comparison between the fractional model and ordinary model, i.e., $\alpha \longrightarrow 1$. The temperature of the ordinary model is higher than that of the fractional model.

Tables 1–3 show some basic findings of the given work. Table 4 depicts a numerical solution for temperature and velocity profiles calculated using the CF and Caputo time derivatives for different values of fractional factor α. It indicates that increasing the fractional factor's value enhances the fluid's temperature and velocity. It suggests that
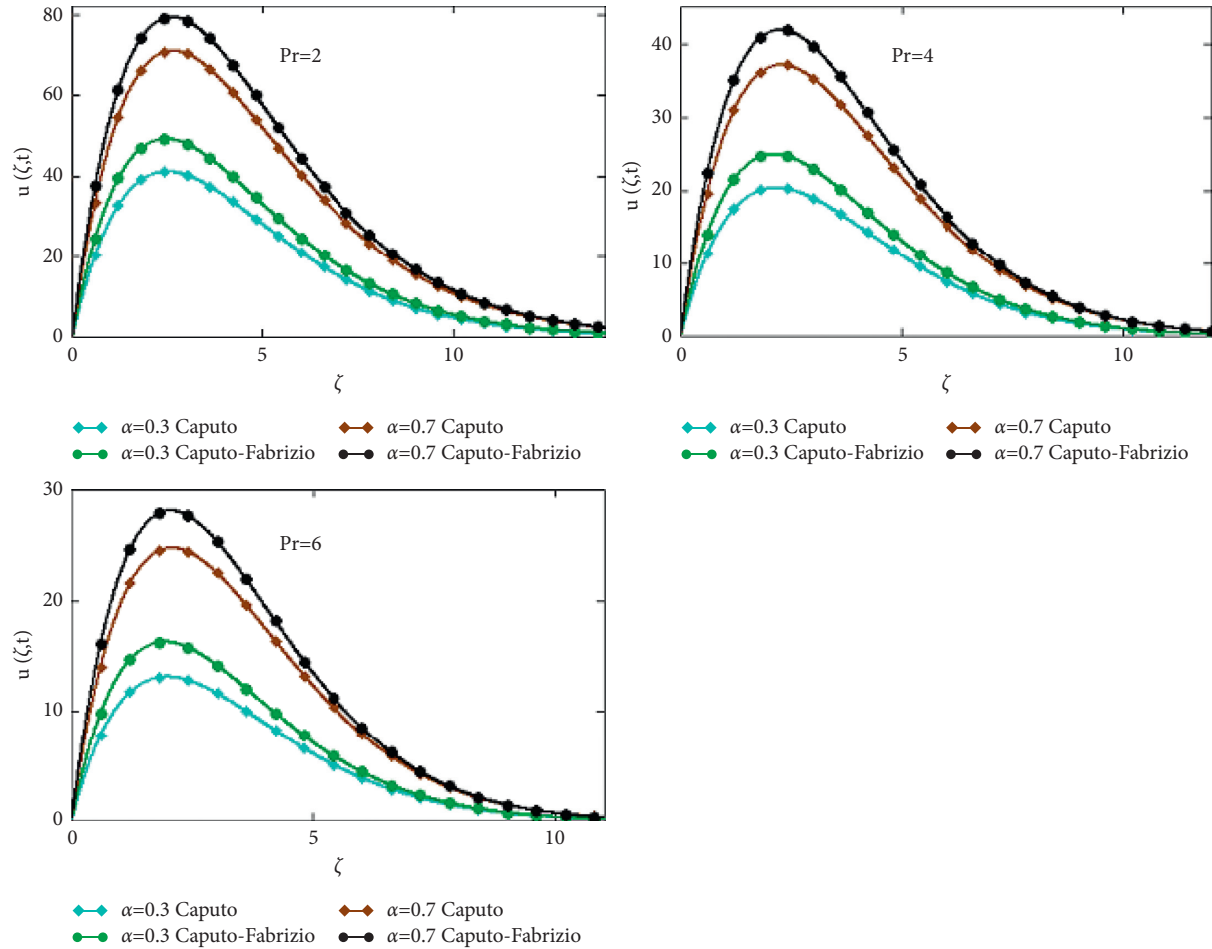
FIGURE 9: Variation of Pr with $Nr = 7, Gr = 10, t = 7$, and $\lambda = 0.1$.

CF has a greater velocity and temperature than Caputo. Table 2 shows the comparisons between various numerical inverse LT algorithms like Stehfest's algorithm and Tzou's algorithm with the exact solution. It verifies the validity and correctness of solutions up to the desired level of precision. Table 3 presents the relationships between the solutions obtained for temperature, velocity, and shear stress using various embedded factors. From this, we can see that the increase of various embedded parameters increases the fluid temperature, velocity, and shear stress except for the Prandtl number which shows the inverse effects from other parameters.

The effect of the velocity curve for the Grashof number is presented in Figure 5. It shows that the enhancement of the value of Gr enhances the velocity of both the models. This behavior is due to the rise in buoyancy force because of temperature gradient. Figure 6 shows the influence of radiation factor Nr on velocity. Clearly, Figure 6 shows that

the velocity of fluid with C and CF variants of fractional derivatives increases due to increasing value of the radiation factor. Figure 7 portrays the behavior of Maxwell fluid factor on velocity field. It shows the same effect as Figure 6. Incrementing the value of the Maxwell fluid factor increments the velocity of the Caputo and Caputo–Fabrizio models. In Figure 8, the impact of time is shown for velocity. It is noted that the fluid velocity increases with the increase in time. The temperature is greater near the plate and decreases as we go away from the plate and finally becomes zero in the free stream region. From Figure 9, we can see that the fluid velocity decreases when the value of Prandtl number Pr increases. Moreover, the enhancement of Pr decreases the thickness of the boundary layer. Figure 10 shows the comparison between the fractional model and ordinary fluid model. It shows that the velocity of the ordinary fluid model, i.e., $\alpha \longrightarrow 1$, is greater than the velocity of the fractional model.
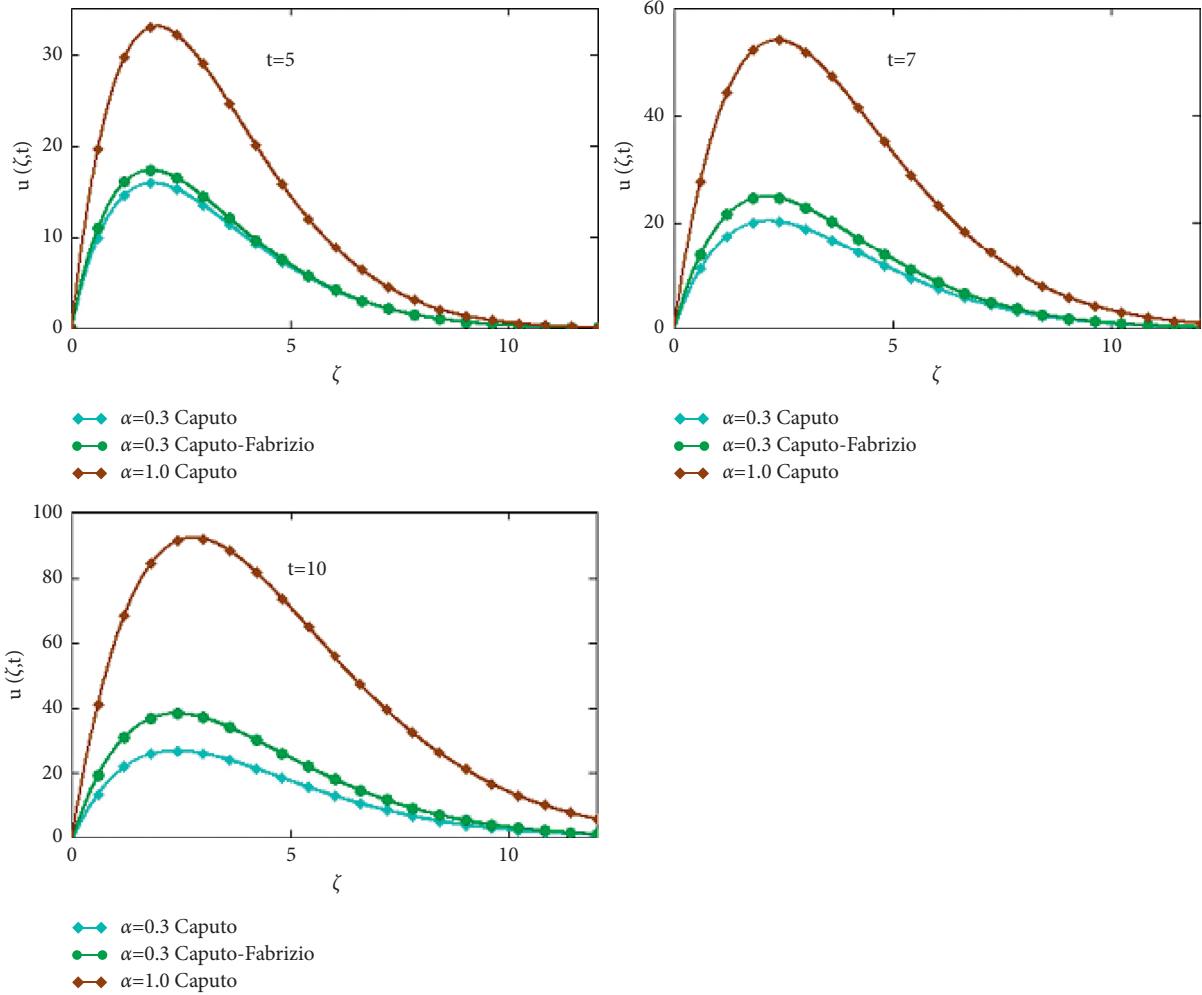
Figure 10: Comparison between fractional model ($t = 7$ and $\lambda = 0.1$) and ordinary model, i.e., $\alpha \longrightarrow 1$.

15. Conclusion

The objective of the present work is to conduct a comparative study of the natural convection flow of fractional Maxwell fluid in the presence of radiation and uniform heat flux. The two fractional derivative definitions are used (C and CF) in the formulation of the problem. The solutions for heat and velocity are obtained through the Laplace transform method. The following are the study's key findings:

(i) The temperature of the fluid increases with increase in the embedded factors like Nr and t.

(ii) Increasing the Prandtl number reduces the fluid's temperature.

(iii) The enhancement of the fluid parameters like Gr, Nr, λ, and t enhances the fluid's velocity for both models, while the Prandtl number shows the adverse effects from other factors.

(iv) Increasing the value of Gr, Nr, and λ increases the shear stress of the fluid, while the Prandtl number has the opposite effect.

Data Availability

No data were used to support this study.

Conflicts of Interest

The authors declare that there are no conflicts of interest.

Acknowledgments

References

[1] M. Sheikholeslami, T. Hayat, and A. Alsaedi, "MHD free convection of Al$_2$O$_3$-water nanofluid considering thermal radiation: a numerical study," *International Journal of Heat and Mass Transfer*, vol. 96, pp. 513–524, 2016.

[2] M. Sheikholeslami and D. D. Ganji, "CVFEM for free convective heat transfer of CuO-water nanofluid in a tilted semi annulus," *Alexandria Engineering Journal*, vol. 56, no. 4, pp. 635–645, 2017.

[3] M. Sheikholeslami and M. M. Rashidi, "Effect of space dependent magnetic field on free convection of Fe_3O_4-water nanofluid," *Journal of the Taiwan Institute of Chemical Engineers*, vol. 56, pp. 6–15, 2015.

[4] M. Sheikholeslami, K. Vajravelu, and M. M. Rashidi, "Forced convection heat transfer in a semi annulus under the influence of a variable magnetic field," *International Journal of Heat and Mass Transfer*, vol. 92, pp. 339–348, 2016.

[5] I. Khan, N. A. Shah, and L. C. Dennis, "A scientific report on heat transfer analysis in mixed convection flow of Maxwell fluid over an oscillating vertical plate," *Scientific Reports*, vol. 7, no. 1, pp. 40147–40211, 2017.

[6] I. Khan, N. A. Shah, Y. Mahsud, and D. Vieru, "Heat transfer analysis in a Maxwell fluid over an oscillating vertical plate using fractional Caputo-Fabrizio derivatives," *The European Physical Journal Plus*, vol. 132, no. 4, pp. 1–12, 2017.

[7] S. Aman, Q. Al-Mdallal, and I. Khan, "Heat transfer and second order slip effect on MHD flow of fractional Maxwell fluid in a porous medium," *Journal of King Saud University Science*, vol. 32, no. 1, pp. 450–458, 2020.

[8] E. U. Haque, A. U. Awan, N. Raza, M. Abdullah, and M. A. Chaudhry, "A computational approach for the unsteady flow of Maxwell fluid with Caputo fractional derivatives," *Alexandria engineering journal*, vol. 57, no. 4, pp. 2601–2608, 2018.

[9] M. B. Riaz, A. Atangana, and N. Iftikhar, "Heat and mass transfer in Maxwell fluid in view of local and non-local differential operators," *Journal of Thermal Analysis and Calorimetry*, vol. 143, no. 1, pp. 1–17, 2020.

[10] C. Fetecau, M. Athar, and C. Fetecau, "Unsteady flow of a generalized Maxwell fluid with fractional derivative due to a constantly accelerating plate," *Computers & Mathematics with Applications*, vol. 57, no. 4, pp. 596–603, 2009.

[11] S. Aman, I. Khan, Z. Ismail, M. Z. Salleh, and Q. M. Al-Mdallal, "Heat transfer enhancement in free convection flow of CNTs Maxwell nanofluids with four different types of molecular liquids," *Scientific Reports*, vol. 7, no. 1, pp. 2445–2513, 2017.

[12] Y. Liu and B. Guo, "Effects of second-order slip on the flow of a fractional Maxwell MHD fluid," *Journal of the Association of Arab Universities for Basic and Applied Sciences*, vol. 24, no. 1, pp. 232–241, 2017.

[13] S. Shateyi and G. T. Marewo, "A new numerical approach of MHD flow with heat and mass transfer for the UCM fluid over a stretching surface in the presence of thermal radiation," *Mathematical Problems in Engineering*, vol. 2013, Article ID 670205, 8 pages, 2013.

[14] A. Mohi, "Effect of MHD on unsteady flow with fractional maxwell model," *Journal of Al-Nahrain University-Science*, vol. 19, no. 2, pp. 130–136, 2016.

[15] M. B. Riaz and N. Iftikhar, "A comparative study of heat transfer analysis of MHD Maxwell fluid in view of local and nonlocal differential operators," *Chaos, Solitons & Fractals*, vol. 132, Article ID 109556, 2020.

[16] K. A. Abro and A. A. Shaikh, "Exact analytical solutions for Maxwell fluid over an oscillating plane," *Science International (Lahore) ISSN*, vol. 27, pp. 923–929, 2015.

[17] M. I. Asjad, N. A. Shah, M. Aleem, and I. Khan, "Heat transfer analysis of fractional second-grade fluid subject to Newtonian heating with Caputo and Caputo-Fabrizio fractional derivatives: a comparison," *The European Physical Journal Plus*, vol. 132, no. 8, pp. 1–19, 2017.

[18] N. Raza and M. A. Ullah, "A comparative study of heat transfer analysis of fractional Maxwell fluid by using Caputo and Caputo-Fabrizio derivatives," *Canadian Journal of Physics*, vol. 98, no. 1, pp. 89–101, 2020.

[19] N. Wang, N. A. Shah, I. Tlili, and I. Siddique, "Maxwell fluid flow between vertical plates with damped shear and thermal flux: free convection," *Chinese Journal of Physics*, vol. 65, pp. 367–376, 2020.

[20] I. Khan, F. Ali, and S. Shafie, "Exact solutions for unsteady magnetohydrodynamic oscillatory flow of a Maxwell fluid in a porous medium," *Zeitschrift für Naturforschung A*, vol. 68, no. 10-11, pp. 635–645, 2013.

[21] L. Zheng, F. Zhao, and X. Zhang, "Exact solutions for generalized Maxwell fluid flow due to oscillatory and constantly accelerating plate," *Nonlinear Analysis: Real World Applications*, vol. 11, no. 5, pp. 3744–3751, 2010.

[22] C. Fetecau, M. Jamil, C. Fetecau, and I. Siddique, "A note on the second problem of Stokes for Maxwell fluids," *International Journal of Non-linear Mechanics*, vol. 44, no. 10, pp. 1085–1090, 2009.

[23] U. Farooq, D. Lu, S. Munir, M. Ramzan, M. Suleman, and S. Hussain, "MHD flow of Maxwell fluid with nanomaterials due to an exponentially stretching surface," *Scientific Reports*, vol. 9, no. 1, pp. 7312–7411, 2019.

[24] M. Jamil, C. Fetecau, and C. Fetecau, "Unsteady flow of viscoelastic fluid between two cylinders using fractional Maxwell model," *Acta Mechanica Sinica*, vol. 28, no. 2, pp. 274–280, 2012.

[25] A. A. Zafar, N. A. Shah, N. Nigar, and N. Nigar, "On some rotational flows of non-integer order rate type fluids with shear stress on the boundary," *Ain Shams Engineering Journal*, vol. 9, no. 4, pp. 1865–1876, 2018.

[26] M. Jamil, K. A. Abro, and N. A. Khan, "Helices of fractionalized Maxwell fluid," *Nonlinear Engineering*, vol. 9, no. 4, p. 191, 2015.

[27] T. Hayat, M. Rashid, A. Alsaedi, and S. Asghar, "Nonlinear convective flow of Maxwell nanofluid past a stretching cylinder with thermal radiation and chemical reaction," *Journal of the Brazilian Society of Mechanical Sciences and Engineering*, vol. 41, no. 2, p. 86, 2019.

[28] M. D. Hisham, A. Rauf, D. Vieru, and A. U. Awan, "Analytical and semi-analytical solutions to flows of two immiscible Maxwell fluids between moving plates," *Chinese Journal of Physics*, vol. 56, no. 6, pp. 3020–3032, 2018.

[29] W. A. Azhar, D. Vieru, and C. Fetecau, "Free convection flow of some fractional nanofluids over a moving vertical plate with uniform heat flux and heat source," *Physics of Fluids*, vol. 29, no. 8, 2017.

[30] J. N. Tokis, "A class of exact solutions of the unsteady magnetohydrodynamic free-convection flows," *Astrophysics and Space Science*, vol. 112, no. 2, pp. 413–422, 1985.

[31] C. Fetecau, S. Akhtar, I. Pop, and C. Fetecau, "Unsteady general solution for MHD natural convection flow with radiative effects, heat source and shear stress on the boundary," *International Journal of Numerical Methods for Heat & Fluid Flow*, vol. 27, no. 6, pp. 1266–1281, 2017.

[32] Samiulhaq, C. Fetecau, I. Khan, F. Ali, and S. Shafie, "Radiation and porosity effects on the magnetohydrodynamic flow past an oscillating vertical plate with uniform heat flux," *Zeitschrift für Naturforschung A*, vol. 67, no. 10-11, pp. 572–580, 2012.